

Generation of quasistanding hypersonic wave in stimulated Brillouin scattering of a broad-band pump

N. F. Bunkin, G. A. Lyakhov, and O. V. Umnova

General Physics Institute of the Russian Academy of Sciences, Vavilova 38, 117942 Moscow, Russia
(Submitted 9 March 1993)

Zh. Eksp. Teor. Fiz. 104, 3287–3296 (October 1993)

We calculate the efficiency of the Brillouin mechanism for the excitation of oppositely directed hypersonic waves by optical pumping, when the pump spectral width exceeds the Stokes frequency shift. This is shown to decrease the threshold for hypersonic cavitation of liquids. We describe an experiment on hypersonic cavitation. Basing on the theoretical results, we estimate the decrease in threshold optical intensity for cavitation in the transition from narrow-band to broad-band pumping. The estimate is in conformity with the experimental data.

1. INTRODUCTION

The theory of stimulated scattering of light by material modes of different nature has been developed in considerable detail, including the effect of finite pump width $\Delta_+^{1,2}$. Clearly the characteristics of the process are decisively dependent on the relative magnitudes of Δ_+ and Δ_r , Ω_0 , ω_p , where Δ_r is the inverse relaxation time of the scattering mode; Ω_0 , the natural frequency of this mode; ω_p , the frequency of optical pumping. For the Brillouin mechanism, which is the strongest one in the majority of liquids³ and which will be the main subject of our analysis, $\Delta_r = \Gamma q^2 = (\zeta + 4\eta/3)q^2/\rho = 10^7 - 10^9 \text{ s}^{-1}$ is the inverse hypersound damping time (ζ and η are the bulk and shear viscosities; ρ is the density of the liquid; $q = \Omega_0/v$ is the wavenumber; v is the speed of sound). As for Ω_0 (the Stokes shift of the scattered light frequency, which is equal to the frequency of the hypersound produced), its value depends on scattering geometry, and we have $\Omega_0 = v\omega_p/c \approx 10^9 - 10^{10} \text{ s}^{-1}$ in the backscattering geometry, which is most efficient. In the transition from virtually monochromatic ($\Delta_+ < \Delta_r$) to more broad-band ($\Delta_r < \Delta_+ < \omega_p$) pumping, stimulated Brillouin scattering efficiency decreases in general, although some special features show up, for instance, a mean-energy threshold associated with steep growth of the Stokes wave intensity. On the other hand, the scattering wave diagram does not change. The pumping excites the oppositely directed Stokes wave and the copropagating hypersonic wave (see Ref. 1).

With further increase in Δ_+ , $\Omega_0 < \Delta_+ < \omega_p$, the wave pattern itself of the interaction should become more complicated. Nonlinear beating of each ω -component of the pump with the oppositely directed Stokes ($\omega - \Omega_0$)-component excites the copropagating hypersonic Ω_0 -component. The Stokes ($\omega - \Omega_0$)-component (quite intense, when the pumping is over the threshold level, which is the necessary condition for the onset of the process in question) in turn can excite oppositely directed hypersound at the same frequency Ω_0 , when interacting with the ($\omega - 2\Omega_0$)-component of the pump (broad-band by assumption). Excitation of such a quasistanding hypersonic

wave can, in particular, lower the threshold for light-induced cavitation in liquids.

The efficiency of quasistanding hypersonic wave excitation in the process of stimulated Brillouin scattering for $\Delta_+ > \Omega_0$ is calculated below using a two-wave generalization of the approach of Pasmanik,⁴ which was applied in the analysis of nonlinear effects in broad-band optical radiation. This extension is also applied to describe scattering of broad-band pumping by a diffusive-type material mode for the example of stimulated temperature scattering.

2. TRANSFORMATION OF SPECTRAL INTENSITIES OF OPPositely DIRECTED OPTICAL WAVES IN STIMULATED BRILLOUIN SCATTERING IN A BROAD-BAND PUMP FIELD

The starting equations for the description of stimulated Brillouin scattering are³

$$\begin{aligned} n^2 \partial_{tt} E - c^2 \partial_{xx} E &= -Y \beta_s \partial_{tt}(pE), \\ \partial_{tt} p - \partial_{xx}(v^2 p + \Gamma \partial_t p - Y|E|^2/8\pi\rho) &= 0, \end{aligned} \quad (1)$$

where E is the electric field strength, p is the sound pressure, n is the refractive index, $Y = \rho \partial \epsilon / \partial \rho$ is the nonlinear coupling parameter, and $\beta_s = (\rho v^2)^{-1}$ is the compressibility of the medium. For the backscattering geometry, the solution of (1) is represented as a superposition of oppositely directed optical and hypersonic waves:

$$\begin{aligned} E &= (E_+/2)\exp(-ik_p x) + (E_-/2)\exp(ik_s x) + \text{c.c.}, \\ p &= (p_+/2)\exp(-iqx) + (p_-/2)\exp(iqx) + \text{c.c.}, \end{aligned} \quad (2)$$

here we have written $q = \Omega_0/v$ and $k_{p,s} = n\omega_{p,s}/c$, $\omega_{p,s}$, Ω_0 are the central frequencies of the pump, scattered wave, and hypersound spectra, respectively. Firstly, we assume that the quasimonochromatic approximation is valid even for $\Delta_+ > \Omega_0$: $\omega_{p,s} \gg \Delta_\pm$, where Δ_\pm are the spectrum widths of the pump wave ($x = -l/2$) and the Stokes wave ($x = l/2$, where l is the length of the scattering volume) incident on the medium. Secondly, we adopt the approximation of strong hypersound damping:

$$al = \Gamma q^2 l / 2v \gg 1,$$

which holds in most liquids (the typical values of α are $\sim 10^3\text{--}10^4 \text{ cm}^{-1}$). This permits equations to be derived for the Fourier-components of the slow amplitudes (2) of the optical field $E_{\pm}(\omega)$ from (1):

$$\begin{aligned} & (32\pi^2c^2k/\omega^2qY^2v\beta_s)\partial_xE_{\pm}(\omega) \\ &= \int \int_{-\infty}^{+\infty} d\omega' d\Omega E_{\pm}(\omega') E_{\mp}^*(\omega' - \Omega) \\ &\quad \times E_{\mp}(\omega - \Omega)/[2\alpha v - i(\Omega_0 - \Omega)] \\ &- \int \int_{-\infty}^{+\infty} d\omega' d\Omega E_{\pm}(\omega') E_{\mp}(\omega + \Omega) \\ &\quad \times E_{\mp}^*(\omega' + \Omega)/[2\alpha v + i(\Omega_0 - \Omega)] \end{aligned} \quad (3)$$

(by virtue of the inequality $\omega_{p,s} \gg \Delta_+ > \Omega_0$ we set $k_p \approx k_s = k$). Thirdly, we assume that the spectrum has Gaussian statistics,

$$cn\langle E_{\pm}(\omega)E_{\mp}(\omega') \rangle / 8\pi = s_{\pm}(\omega)\delta(\omega - \omega').$$

This makes it possible to uncouple the fourth-order correlators when averaging (3):

$$\begin{aligned} & \pm(\pi cn^3/kqav^2Y^2\beta_s)\partial_x s_{\pm} \\ &= \int_{-\infty}^{+\infty} d\Omega [s_{\mp}(\omega - \Omega) - s_{\mp}(\omega + \Omega)]/ \\ &\quad \times [(2\alpha v)^2 + (\Omega_0 - \Omega)^2]. \end{aligned} \quad (4)$$

Finally, the basic assumption

$$\partial \ln s_{\pm}(\omega) / \partial \omega \ll \Omega_0^{-1}$$

allows us to restrict ourselves to the lowest-order terms in the expansions:

$$s_{\pm}(\omega \pm \Omega) \approx s_{\pm}(\omega) \pm \Omega \partial_{\omega} s_{\pm}(\omega).$$

As a result, Eqs. (4) go over to the system

$$S_{\pm} = (n^{-3}c^{-1}qkvY^2\beta_s J) s_{\pm}, \quad X = x/l, \quad W = (\omega - \omega_p)/\Omega_0$$

after the normalization

$$\partial_X S_{\pm} = \pm S_{\pm} \partial_W S_{\mp}. \quad (5)$$

The boundary conditions ($X = -1/2, X = 1/2$), are imposed at the opposite ends of the medium, which is the main difficulty in analyzing (5). We assume for definiteness that

$$S_{\pm}(\mp 1/2, W) = S_{\pm}^0 \exp(-W^2/D_{\pm}^2). \quad (6)$$

Returning now from (4) to (1), we obtain that the intensities of the hypersound waves

$$\mathcal{T}_{\pm} = |p_{\pm}|^2/2\rho v$$

result from direct integration (in the dimensional variables):

$$\mathcal{T}_{\pm}(x) = \pi q^2 Y^2 / 4n^2 c^2 \rho \alpha \int_{-\infty}^{+\infty} d\omega s_{\pm}(\omega, x) s_{\mp}(\omega - \Omega_0, x). \quad (7)$$

Equation (5) has an infinite number of integrals:

$$\begin{aligned} \partial_X \int d\omega \ln S_{\pm} &= \partial_X \int d\omega (S_{+} - S_{-}) \\ &= \partial_X \int d\omega (S_{+}^2 - 4S_{+}S_{-} + S_{-}^2) \dots = 0. \end{aligned}$$

Formally, it can be exactly integrated by the hodograph method, however, it is hard to extract the desired quantitative output from the resulting integral equations.

Let us linearize (5) in the variables $\ln(S_{\pm}/S_{\pm}^0)$. This approximation is less artificial than assuming the field to be given, and allows partially for pump depletion. As analysis shows, it is very accurate when describing the energy-carrying central regions of the S_{\pm} spectra, but becomes less so in the wings of the spectrum, which contain a small fraction of the energy. This is a special analog of the “paraxial” approximation in the description of the diffractive spreading of beams. The solution of Eqs. (5) linearized in this way gives (in dimensional variables)

$$s_{\pm}(\pm l/2, \omega) = s_{\pm}^0 \exp[\mp G_{\pm} - (\omega - \omega_p + \delta_{\pm})^2/\Delta_{\pm}^2]. \quad (8)$$

Here

$$G_{\pm} = s_{\mp}^0 s_{\pm}^0 (1 - \xi) (\Delta_{\pm} \Omega_0 / \tilde{S} \Delta_{\pm}^2)^2$$

are the amplification coefficients,

$$\delta_{\pm} = (s_{\mp}^0 \Omega_0 / \tilde{S}) (\Delta_{\pm} / \Delta_{\mp})^2$$

are the frequency shifts, and we have written

$$\xi = (s_{-}^0 / s_{+}^0) (\Delta_{+} / \Delta_{-})^4, \quad \tilde{S} = cn^3/qkvY\beta_s^2 l.$$

Thus, stimulated Brillouin scattering of a broad-band pump ($\Delta_{\pm} \gg \Omega_0$) does not alter the spectrum widths of the pump and the counter wave. The spectra undergo a shift as a whole to the Stokes region by δ_{\pm} (Fig. 1). If $s_{+}^0 > s_{-}^0 (\Delta_{+} / \Delta_{-})^4$ ($\xi < 1$) holds, then the laser radiation energy is transferred to the oppositely propagating signal with growth rate $G_{-} \sim (I_{+}/l)^2$, where $I_{+} = s_{+} \Delta_{+}$ is the pump intensity. In this case, the shift of the backward signal spectrum is larger than the shift of the pump spectrum:

$$\delta_{-} / \delta_{+} = \xi^{-1} > 1.$$

Now the conditions for validity of the linear approximation in $\ln(S_{\pm}/S_{\pm}^0)$ can be specified:

$$\delta_{\pm} < \min(\Delta_{+}, \Delta_{-}).$$

Note that this linearization preserves the integrals $\int d\omega \ln S_{\pm}$ for any relation between Δ_{+} and Δ_{-} . The other integrals are preserved with higher accuracy as the ratio Δ_{+}/Δ_{-} approaches unity.

3. HYPERSONIC CAVITATION IN A BROAD-BAND OPTICAL FIELD-EXPERIMENT

In this experiment, (with the layout of Ref. 5), a XeCl laser was used ($\lambda = 308 \text{ nm}$, pulselength $\tau = 20 \text{ ns}$, energy up to 50 mJ) with oscillation linewidth of 15 cm^{-1} , i.e., considerably larger than the Stokes shift (0.1 cm^{-1}). The pump spectrum could be narrowed down or, more pre-

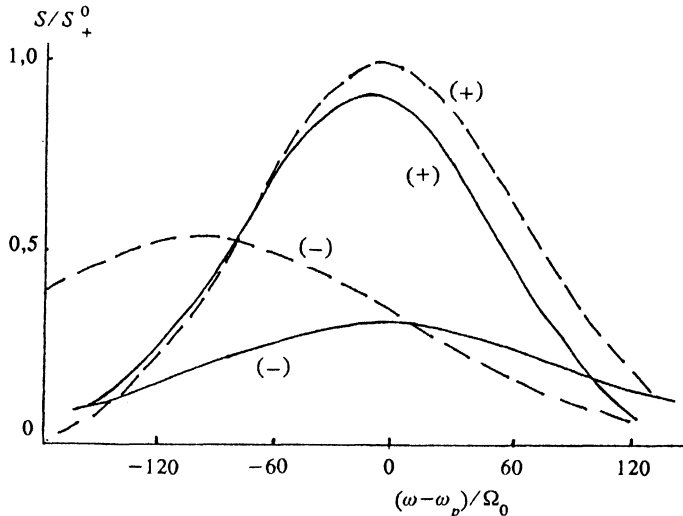


FIG. 1. Spectral densities of the pump S_+ and the backward wave S_- at the output ($x=l/2$, solid lines) and the input ($x=-l/2$, dashed lines) of the scattering medium at $s_+^0=1\text{ J/cm}^2=3s_-^0$, $\tilde{S}=2 \cdot 10^{-2}\text{ J/cm}^2$, $\Delta_+/\Omega_0=\Delta_-/\Omega_0=100$, $(G_+=7.5 \cdot 10^{-2}, G_-=5.6 \cdot 10^{-1}, \delta_+/\Omega_0=6, \delta_-/\Omega_0 \approx 100)$.

cisely, thinned out. Two lines were obtained of width $<0.1\text{ cm}^{-1}$ with a frequency interval of $\sim 0.7\text{ cm}^{-1}$. The pulse energy in this case was $\sim 10\text{ mJ}$.

A laser radiation pulse was directed using lenses to a cell containing the liquid being investigated. Once a certain intensity $I_+^0=I_{th}$ was obtained, the liquid cavitated along the length of the waist: tracks emerged, consisting of floating bubbles. As this took place, the beam cross section increased abruptly (by approximately a factor of five) due to scattering from the bubble track. Concurrently with cavitation, a backscattered signal appeared with an intensity $I_- \sim 0.1 I_{th}$. At the same pumping intensity (and even at intensities one or two orders of magnitude higher), cavitation was absent if the spectrum was thinned out. In this case, the backscattered signal intensity was $I_- < I_+^0$.

A thin cell with a fluorescent screen behind it was used to study the dynamics of bubble formation. The cell thickness was $20\text{ }\mu\text{m}$, i.e., much less than the waist length. Once I_{th} was attained, cavitation bubbles appeared along the whole beam path in the cell. The bubbles were imaged on the fluorescent screen along with the accompanying spherical waves. The image on the screen corresponding to cavitation appeared during the course of the laser pulse, i.e., the bubbles had a chance to form over an interval of $<20\text{ ns}$. Such rapid growth can be explained in the frameworks of the bubble-cluster model of gases dissolved in a liquid.⁶

The experimental parameters for the observations of cavitation in water were: $I_+^0=s_+^0\Delta_+=10^4-10^6\text{ MW/cm}^2$ (in the waist of the beam), $l=0.5\text{ cm}$, $\Delta_+=3 \cdot 10^{12}\text{ s}^{-1}$, $\omega_0=6 \cdot 10^{15}\text{ s}^{-1}$, $\Omega_0=2 \cdot 10^{10}\text{ s}^{-1}$. Under these conditions we have $\tilde{S} \approx 2 \cdot 10^{-2}\text{ J/cm}^2$, $s_+^0=0.01-1\text{ J/cm}^2$, and $\xi \ll 1$, since the spectral power density of the seed of the Stokes wave is small, $s_-^0 \ll s_+^0$. The spectrum shift of the scattered wave is less than the pumping spectrum width ($\delta_- \ll \Delta_+$) at $(\Delta_-/\Delta_+) \ll (\Delta_+^3 \tilde{S}/\Omega_0 \alpha v)^{1/2} \approx 1-10$. Hence, we have an upper bound for the scattering growth rate, $G_- \ll 0.1-10$. Note that the scattering growth rate for monochromatic pumping under similar conditions is

$$G_m=I_+^0/4\alpha v \tilde{S}=G_-^{1/2}(\Delta_+/4\Delta_- \Omega_0 \alpha v) \approx 10^3-10^5,$$

i.e., much greater than G_- . Indeed, in the experiment, the ratio of the pumping intensity and the backward wave intensity was a few tens of percents in monochromatic light scattering and no more than a few percent in scattering of a broad-band pump.

4. CALCULATION OF HYPERSOUND INTENSITY AND EVALUATION OF THE CAVITATION THRESHOLD

To estimate the feasibility of inducing cavitation owing to this effect, we shall calculate the intensities of the oppositely propagating hypersonic waves for the point $x=-l/2$, in whose vicinity ($x_m-l/2=(\alpha l)^{-1} \approx 10^{-2}-10^{-3} \ll 1$) they have maxima. It follows from (7), if (8) is accounted for, that

$$\begin{aligned} \mathcal{T}_\pm(-l/2)=&\pi^{3/2}\Omega_0^3 Y^2(\Delta_+\Delta_-)^{1/2}/4(cn)^2 v^2 \rho \alpha \\ &\times (\Delta_+^2 + \Delta_-^2)^{1/2} s_+^0 s_-^0 \\ &\times \exp[(s_+^0 \Delta_- \Omega_0 / \tilde{S} \Delta_+^2)^2(1-\xi)] \\ &- \Omega_0^2(s_+^0 \Delta_-^2 / \Delta_+^2 \tilde{S} \mp 1)^2 / (\Delta_+^2 + \Delta_-^2), \end{aligned} \quad (9)$$

the hypersound linewidth does not change in a broad-band field and is $\Delta_r=\Gamma q^2$. The ratio of the intensities of the forward and the backward hypersound is thus equal to

$$\begin{aligned} \mathcal{T}_-(-l/2)/\mathcal{T}_+(-l/2) \\ = \exp[-4s_+^0 \Omega_0^2 / \Delta_+^2 (\Delta_+^2 + \Delta_-^2 + 1) \tilde{S}]; \end{aligned} \quad (10)$$

it tends to unity with pumping spectrum broadening (Fig. 2). For the conditions of the experiment with water, an estimate follows from (9):

$\mathcal{T}_-(-l/2) \approx \mathcal{T}_+(-l/2) \approx (10^2-10^6)(I_-^0/I_+^0)\text{ W/cm}^2$, where I_-^0/I_+^0 is the ratio of the pump and the initial noise intensities at the rear wall of the cell. The spread in the estimate is associated with the possibility of varying the conditions of pump beam focusing (the length and the radius of the waist) and reflection.

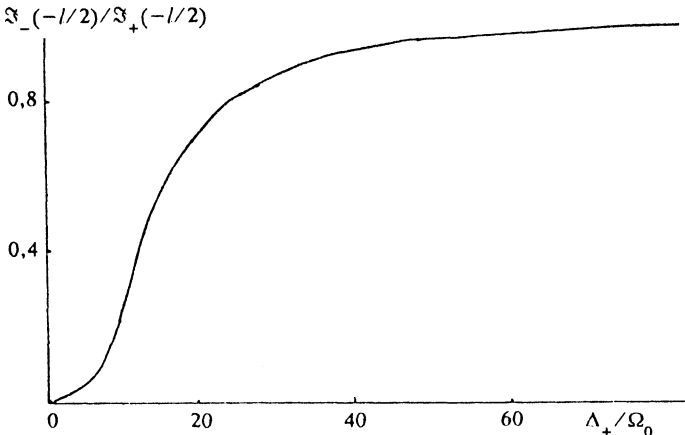


FIG. 2. Ratio of the backward and the forward hypersound intensities as a function of the relative spectral width of the pump.

The experimental value of the cavitation threshold for the hypersonic (gigahertz) range investigated is unknown. For ultrasonic frequencies (the Megahertz range) it is $\mathcal{T}_c \approx 1 \text{ W/cm}^2$ (Ref. 7). The approximation of nearly quadratic growth of the minimum (for cavitation seeds with resonant dimensions) threshold value of \mathcal{T}_c with frequency growing in the hypersonic range gives $\mathcal{T}_c(\Omega_0 \approx 10^{10} \text{ Hz}) > 1 \text{ MW/cm}^2$, exceeding the intensity $\mathcal{T}_m \approx 10^{-3} \text{--} 10^0 \text{ MW/cm}^2$ of the hypersound generated in the experiment with a thinned out pump spectrum. A qualitative explanation for the appearance of cavitation in the weaker field of a standing hypersonic wave ($\mathcal{T}_\pm \approx 10^{-6} \text{--} 10^{-2} \text{ MW/cm}^2$ if $I_-^0/I_+^0 \approx 10^{-2}$) may be given by invoking the concept of the cluster mechanism of nucleation:⁶ the gas bubbles ($R_0 \approx 10^{-4} \text{--} 10^{-3} \text{ cm}$) observed in the experiment are formed by the coalescing of clusters of stable microbubbles-bubstones ($R_0 \approx 10^{-7} \text{ cm}$). The ratio of the forces of radiation pressure acting on a particle of small radius ($qR \ll 1$) in standing (\mathcal{T}_s) and traveling (\mathcal{T}_t) acoustic waves ranges from $(\mathcal{T}_s/\mathcal{T}_t)(qR)^{-1}$ for compressible bubbles to $(\mathcal{T}_s/\mathcal{T}_t)(qR)^{-3}$ for the model of incompressible particles whose density is equal to the density of water.⁸ For the model of Ref. 6, $(qR_0) \approx 10^{-2}$, so cluster coalescence proceeds more efficiently in a standing wave than in a traveling wave in the limit $\mathcal{T}_s/\mathcal{T}_t = \mathcal{T}_\pm/\mathcal{T}_m \geq 10^{-2} \text{--} 10^{-6}$, depending on compressibility of microbubbles. The calculated value of $\mathcal{T}_\pm/\mathcal{T}_m \approx 10^{-3} \text{--} 10^{-2}$ falls just within this range. Apparently, a more detailed calculation of bubston cluster coalescence threshold requires that the dependence of bubston compressibility on frequency and their interaction potential be included.

Note that this explanation of cavitation of a liquid in a broad-band pumping field differs from the theory of Ref. 10, where the effect is ascribed to induced optical coalescence of clusters due to short (of the order of several picoseconds) energy spikes resulting from multimode interference. The amplitude of these spikes may be considerably greater than the mean energy in a pulse and higher than the induced optical coalescence threshold. However, the appearance of giant spikes is a stochastic process, therefore, cavitation should be expected to be sporadic. But in the experiment the cavitation was quite regular. Investiga-

tion of the effect of laser pulse energy fluctuations on cavitation should be a subject of a separate work.

5. STIMULATED SCATTERING OF A BROAD-BAND PUMP BY A DIFFUSIVE MATERIAL MODE

The universal form of the reduced elliptic system of Eq. (5) describing variations in optical field intensities in the process of stimulated Brillouin scattering is indicative of their wider applicability (provided that the obvious generalization is made). Indeed, the same equations describe stimulated scattering by diffusive modes like the thermal mode. Generally speaking, the characteristic shift is considerably smaller here than under the action of wave-scattering mechanisms. Therefore, the approximation proposed in Sec. 2 is more accurate here.

The original equations for the description of stimulated thermal scattering of light, allowing for thermal nonlinearity light wave (in the plane-wave approximation) are:³

$$(c/n\omega_0)^2 \partial_{xx} E + E = -2\gamma TE, \quad (11)$$

$$\partial_t T - \chi \partial_{xx}^2 T - \chi \nabla_1^2 T = (8\pi\delta_0/(cn)\rho c_p) |E|^2.$$

Here, T is the light-induced increase in the medium temperature $\gamma = \partial \ln n / \partial T$, χ is the thermal diffusivity, and c_p is the heat capacity. For oppositely directed optical waves (2) with frequency ω_0 (here the frequency shift in the basic approximation is set to zero, $k_p = k_s = k = \omega_0 n/c$) and a temperature grating

$$T = T_0 + T_1 \exp(-2ikx) + T_1^* \exp(2ikx),$$

we average (11) over a spatial period $2\pi/k$. Under the assumption that a uniform temperature profile is established primarily due to transverse diffusion ($\chi \nabla_1^2 T_0 \approx (\chi/a^2) T_0$, where a is the pump beam radius, $a \ll l$) and the spatial modulation of temperature T_1 is bounded by longitudinal diffusion ($\chi \partial_{xx} T_1 \approx \chi(k/2\pi)^2 T_1$), this gives reduced equations for E_\pm, T_i ($i=0, 1$):

$$\begin{aligned}\partial_x E_{\pm} &= \mp i(n\omega_0\gamma/c)(E_{\pm}T_0 + E_{\mp}T_{1,2}), \\ \partial_t T_i + \Delta_r^i T_i &= (8\pi\delta_0/cn\rho c_p)[\delta_{0i}(E_+E_+^* + E_-E_-^*) \\ &\quad + \delta_{1i}E_+E_-^*]\end{aligned}$$

(here δ_{ik} is the Kronecker symbol and $\Delta_r^0 = \chi a^{-2}$, $\Delta_r^1 = \chi(a^{-2} + (2\pi/k)^{-2})$ are the inverse relaxation times for T_0 and T_1). Further, for the equations for the pump and the backward wave spectral intensities, under the assumptions made above we have

$$\begin{aligned}\partial_x s_{\pm}(\omega) &= \mp(n\omega_0\gamma\delta_0/4\pi^2c\rho c_p)s_{\pm}(\omega) \\ &\times \left[\int_{-\infty}^{+\infty} \Omega s_{\pm}(\omega - \Omega) d\Omega / (\Omega^2 + (\Delta_r^0)^2) \right. \\ &\quad \left. \times \int_{-\infty}^{+\infty} \Omega s_{\mp}(\omega - \Omega) d\Omega / (\Omega^2 + (\Delta_r^1)^2) \right].\end{aligned}$$

In the broad-spectrum limit, $\partial \ln s_{\pm}(\omega) / \partial \omega \ll (\Delta_r^{0,1})$, we again retain the lowest-order terms in the expansions $s_{\pm}(\omega - \Omega) \approx s_{\pm}(\omega) - \Omega \partial_{\omega} s_{\pm}(\omega)$, and make the substitution

$$\Omega / (\Omega^2 + (\Delta_r^{0,1})^2) \rightarrow \pi\delta(\Omega - \Delta_r^{0,1}) - \pi\delta(\Omega + \Delta_r^{0,1}).$$

As a result, we obtain the equations

$$\partial_x S_{\pm} = \pm S_{\pm} [(\Delta_r^0/\Delta_r^1)\partial_w S_{\pm} + \partial_w S_{\mp}] \quad (12)$$

with boundary conditions (6) for the normalized spectral intensities

$$S_{\pm} = (k\omega_0\gamma\delta_0 l / 4\pi^2 c \rho c_p) s_{\pm}$$

in the coordinates $X = x/l$ and $W = (\omega - \omega_0)/\Delta_r^{0,1}$.

If $S_+^0/S_-^0 \ll (ka/2\pi)^2$, then stimulated scattering prevails, and the variations of the spectral intensities are described by the system (5) as well as in stimulated Brillouin scattering. This is valid, of course, only if the pump spectrum is broad enough: $\Delta_+ > \Omega_0$ and $\Delta_+ > \Delta_r^{0,1}$, respectively. If $S_+^0/S_-^0 > (ka^2/2\pi)^2$, then the thermal nonlinearity of the pump dominates, and Eq. (12) gives a single equation of the "shock-wave" type.⁴

6. CONCLUSION

Thus, the integrable nonlinear equations obtained in Secs. 1 and 4 describe transformations of the spectral intensities of a broad-band pump, S_+ , and an oppositely directed optical wave, S_- , in a nonlinear medium for both reactive ($\Delta_+ > \Omega_0$, stimulated Brillouin scattering) and active ($\Delta_+ > \Delta_r$, stimulated temperature scattering) interaction mechanisms. The broad-band character of the pumping alters the wave diagram for stimulated scattering, namely, two oppositely directed hypersonic beams are formed (with their spectral width remaining the same, $\sim 2av$), the intensity ratio $\mathcal{T}_+(-l/2)/\mathcal{T}_-(l/2)$ of the

forward and the backward hypersonic waves increases with the pump spectral width Δ_+ growing according to the law

$$\ln [\mathcal{T}_-(-l/2)/\mathcal{T}_+(-l/2)] \sim -(\Omega_0/\Delta_+)^2$$

and, as the estimates show, it becomes almost equal to unity under experimental conditions typical of liquids.

The pump and the backward wave spectra retain their initial Gaussian shape and shift as a whole toward the Stokes region. The backward wave frequency shift, $\delta_- \sim s_+^0$, is an order of magnitude larger than the pumping spectrum shift, $\delta_+ \sim s_-^0$, and is $(50-100)\Omega_0$ under typical conditions.⁵ The scattering growth rate grows according to the quadratic law with the length l and the intensity $I_+^0 = s_+^0 \Delta_+$ increasing: $G \sim (I_+^0 l)^2$ ($G_m \sim I_+^0 l$ for a monochromatic pumping) but decreases with the spectrum width Δ_+ increasing as $G \sim (\Delta_+/\Omega_0)^{-2}$. A typical estimate gives $G_- \approx 0.01-10$, which is one or two orders of magnitude lower than G_m . The estimates show that hypersonic cavitation of a liquid is excited more efficiently by stimulated scattering of broad-band light, since the standing hypersonic wave is comparable in its cavitation efficiency to a traveling wave whose intensity is from two to six orders of magnitude higher, depending on the elastic properties of the bubbles. Our calculation gives

$$\mathcal{T}_-(-l/2) \approx \mathcal{T}_+(-l/2) \ll 10^{-2} \text{ MW/cm}^2,$$

which is two or three orders of magnitude lower than the intensity $\mathcal{T}_m(-l/2)$ of hypersound excited by a monochromatic pumping of the same intensity.

The theory presented in Secs. 1 and 4 is also of interest for the phenomenologically similar processes of stimulated scattering of sound by diffusive material modes.⁹ This effect has not yet been observed because of strong competing processes (shock wave generation, self-focusing, sound-induced fluxes). Additional prospects associated with the use of a narrow-band probing sound wave are attractive here (Eqs. (9) and (10) for $\Delta_- \ll \Delta_+$).

¹S. A. Akhmanov, Yu. E. D'yakov, and A. S. Chirkin, *Introduction to Statistical Radiophysics and Optics* [in Russian], Nauka, Moscow, 1981.

²B. Ya. Zel'dovich, N. F. Pilipetskii, and V. V. Shkunov, *Principles of Phase Conjugation*, [Springer, New York, 1985].

³V. S. Starunov and I. L. Fabelinskii, *Usp. Fiz. Nauk* **98**, 441 (1969) [*Sov. Phys. Usp.* **12**, 463 (1970)].

⁴G. A. Pasmanik, *Zh. Eksp. Teor. Fiz.* **66**, 490 (1974) [*Sov. Phys. JETP* **39**, 234 (1974)].

⁵N. F. Bunkin and V. B. Karpov, *Pis'ma Zh. Eksp. Teor. Fiz.* **52**, 669 (1990) [*Jetp Lett.* **52**, 18 (1990)].

⁶N. F. Bunkin and F. V. Bunkin, *Zh. Eksp. Teor. Fiz.* **101**, 512 (1992) [*Sov. Phys. JETP* **74**, 271 (1992)].

⁷L. D. Rozenberg (ed.), *High-Intensity Ultrasonic Fields* Plenum, New York, 1971.

⁸V. A. Krasil'nikov and V. V. Krylov, *Introduction to Physical Acoustics* [in Russian], Nauka, Moscow, 1984.

⁹F. V. Bunkin and G. A. Lyakhov, *Trudy FIAN* **156**, 3 (1984).

¹⁰N. F. Bunkin and F. V. Bunkin, *Laser Physics* **3**, 63 (1993).

Translated by A. M. Mozharovsky